

# Parameters Affecting the Performance of a Residential-Scale Stationary Fuel Cell System

Mark W. Davis  
e-mail: mark.davis@nist.gov

A. Hunter Fanney

Michael J. LaBarre

Kenneth R. Henderson

Brian P. Dougherty

National Institute of Standards and Technology,  
Heat Transfer and Alternative Energy Systems  
Group,  
Gaithersburg, MD 20899-8632

*Researchers at the National Institute of Standards and Technology have measured the performance of a residential fuel cell system when subjected to various environmental and load conditions. The system, which uses natural gas as its source fuel, is capable of generating electrical power at three nominal power levels (2.5, 4.0, and 5.0 kW) while providing thermal energy for user-supplied loads. Testing was conducted to determine the influence of ambient temperature, relative humidity, electrical load, and thermal load on system performance. Steady-state and transient tests were conducted. The steady-state tests were performed in accordance with the American Society of Mechanical Engineering Fuel Cell Power Systems Performance Test Code (PTC-50) for fuel cell power systems. The results of the investigation are being used to develop a proposed rating procedure for residential fuel cell units. [DOI: 10.1115/1.2713767]*

## Introduction

As fuel cell technology matures, numerous applications are emerging. One such application is the installation of a stationary fuel cell at a residence or small business. This application is perceived to have the potential to mature faster than fuel cells for transportation due to the ready supply of fuel (natural gas pipelines or propane storage tanks), the relatively lax constraint on size and weight of the systems, and the relatively high price of electrical power [1–3].

In theory, fuel cells offer an electrical efficiency 40% to 50% [3]. In practice, however, the additions of a reformer to convert the natural gas or propane to hydrogen and an inverter to convert the dc electricity to ac power significantly reduce the electrical efficiency of the overall system. Several field demonstrations of residential fuel cell systems [4–7], for example, have reported net electrical efficiencies between 20% and 30%. Given these practical levels for electrical efficiencies, utilization of only the electrical energy generated by a fuel cell system may be insufficient to justify the initial investment. Consequently, the economic feasibility of fuel cells in residential and small commercial applications will often depend upon what fraction of the fuel cell's considerable heat generation can also be used in meeting the building's thermal (e.g., domestic hot water, space heating) loads.

Currently, consumers lack a tool to determine the economic feasibility for residential fuel cell systems. ASME PTC-50 [8] for fuel cell power systems provides an effective procedure for manufacturers to measure the steady-state efficiency of their fuel cell systems. It does not, however, specify the test conditions nor present a methodology that could be used to predict annual performance under varying environmental and load conditions.

A rating procedure under development at NIST will provide a metric for consumers to judge the economic impact of a residential or small commercial fuel cell system. The rating procedure will account for the primary operational parameters that affect the system's performance and interaction with the electrical and thermal loads. Ultimately, the rating procedure will be submitted to a

consensus standards organization for consideration, since NIST does not issue standards, test methodologies, or rating procedures on its own.

This paper presents the extensive testing performed at NIST on a residential-scale fuel cell system that provides a baseline for the development of the rating procedure. Results from further testing of different residential-scale fuel cell systems will be used to expand and refine, as appropriate, the draft rating procedure. Testing to date shows that the electrical load, thermal load, and environmental conditions can significantly affect the measured performance. Additionally, the data presented in this paper, which show a wide range of measured thermal output according to the fluid temperature and flow rate, emphasize the importance of a rating procedure based upon real-world thermal loads.

## Test Facility

All tests were performed in the NIST Residential Fuel Cell Test Facility on a stationary proton exchange membrane fuel cell system that was purchased from a major manufacturer. The fuel cell system included a natural gas reformer and an ac inverter for the electrical output. It produced up to 5 kW of ac electrical power and more than 9 kW of thermal power. The facility (Fig. 1) was constructed to test residential-scale fuel cell systems over a wide range of environmental, electrical, and thermal loads [9]. The test facility permits the measurement of a system's fuel consumption, fuel energy content, electrical energy output, and thermal energy output. Operational parameters that can be controlled during a test include: the temperature and relative humidity of the air surrounding the fuel cell, the electrical output of the fuel cell, and the flow rate and temperature of the fluid used to extract the thermal load from the fuel cell. As shown in Fig. 1, the fuel cell unit was installed in the test chamber that mimics outdoor weather conditions.

**Control.** The facility allows the range of control that is listed in Table 1. The electrical load can be supplied to a bank of computer-controlled ac loads or to the local utility grid. When the electrical load is directed to the ac loads, the output power, current, or resistance, and the power factor or crest factor are user-selectable. To maintain a steady ambient environment, the fuel cell system is installed within an environmental chamber that controls both the relative humidity and ambient temperature. The thermal energy produced by the fuel cell is extracted using a mixture of 35% propylene glycol and 65% water by volume fraction as a heat transfer fluid, which allows for testing at ambient tem-

Submitted to ASME for publication in the JOURNAL OF FUEL CELL SCIENCE AND TECHNOLOGY. Manuscript received: March 11, 2005; final manuscript received May 8, 2006. Review conducted by Ken Reifsnider. Paper presented at the 3rd International Fuel Cell Science Engineering and Technology Conference (FUEL-CELL2005), Ypsilanti, MI, May 23–25, 2005.

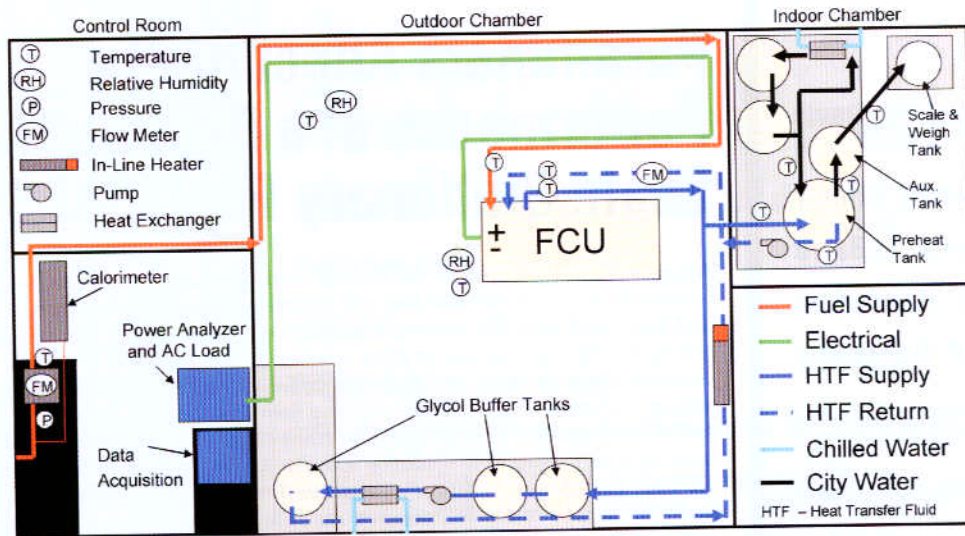


Fig. 1 Schematic of NIST Residential Fuel Cell Test Facility

perature below freezing. The heat transfer fluid flow rate is controlled using two variable-speed pumps in series. Two chilled-water cooled, flat plate heat exchangers and a 3 kW in-line heater control the heat transfer fluid temperature in a fluid conditioning loop.

In lieu of controlling the heat transfer fluid temperature, the fluid can be diverted from the fluid conditioning loop to a simulated residential domestic hot water system. In this arrangement, the fluid transfers heat to a 0.30 m<sup>3</sup> (80 gal) preheat tank through an integral heat exchanger. When a hot water load is imposed, water is withdrawn from the preheat tank through a 0.19 m<sup>3</sup> (50 gal) auxiliary electric water heater into a weigh tank and scale, which records the water volume drawn. Water is withdrawn in accordance with the United State's Department of Energy's (DOE) residential water heater test procedure [10]. Make-up water into the preheat tank is also temperature controlled.

**Measurement.** The test facility measures the fuel energy consumed and the electrical and thermal energy produced by the fuel cell. The uncertainties for each measurement and the associated instruments are shown in Table 2. The fuel energy consumption is measured using a dry-type natural gas meter. A calorimeter continually measures the energy content of the gas. The electrical energy output is measured directly with a power analyzer. For the thermal energy output, the flow rate of the heat transfer fluid is measured with both a turbine and magnetic flow meter for redundancy. The temperature difference imparted to the fluid by the fuel cell is measured using a pair of platinum-resistance thermometers. The density and specific heat of the glycol-water mixture are calculated using previously derived correlations between these properties and the fluid temperature.

Equations (1)–(6) relate individual measurements with the energy flows to/from the fuel cell and the respective efficiencies. All efficiencies reported in this paper are calculated using the higher heating value of natural gas, which is consistent with other appli-

ance rating procedures. The difference between the higher and lower heating value of natural gas is approximately 11%. The lower heating value efficiencies can be approximated by multiplying the reported values by 1.11.

$$E_{\text{fuel}} = \sum_i \left( V_{\text{fuel},i} \cdot \frac{298.15 \text{ K}}{101325 \text{ Pa}} \cdot \frac{P_{\text{fuel},i}}{T_{\text{fuel},i}} \cdot e_{\text{fuel},i} \right) \quad (1)$$

$$E_{\text{electrical}} = \sum_i [E_{\text{electrical},i}] \quad (2)$$

$$E_{\text{thermal}} = \sum_i [(V_{\text{HTF},i}) \times (\rho_{T_{\text{avg},i}}) \times (c_{p,T_{\text{avg},i}}) \times (T_{\text{outlet},i} - T_{\text{inlet},i})] \quad (3)$$

$$\eta_{\text{electrical}} = \frac{E_{\text{electrical}}}{E_{\text{fuel}}} \cdot 100\% \quad (4)$$

$$\eta_{\text{thermal}} = \frac{E_{\text{thermal}}}{E_{\text{fuel}}} \cdot 100\% \quad (5)$$

$$\eta_{\text{overall}} = \eta_{\text{electrical}} + \eta_{\text{thermal}} \quad (6)$$

Table 1 Control parameter ranges

Control Parameter	Minimum	Maximum
Electrical power	0.1 kW	6 kW
Ambient temperature	-10°C	40°C
Relative humidity	20%	75%
Fluid flow rate	5 l/min	40 l/min
Fluid temperature	8°C	65°C

Table 2 Measured uncertainties

Measurement	Expanded Uncertainty ( $k=2$ )
Fuel Energy	0.6%
Natural gas flow meter	0.2%
Calorimeter	0.55%
Fuel temperature	0.3°C
Fuel Pressure	0.8%
Electrical Energy	0.7%
Electrical Efficiency	0.2% (i.e., 20% ± 0.2%)
Thermal Energy	3.5%
Magnetic flow meter	1.2%
Temperature	0.05°C
Density	1.0%
Specific heat	3.0%
Thermal Efficiency	4.0% (i.e., 35% ± 4.0%)

**Table 3 Grid-interconnected electrical efficiency four-test bracket**

Load fraction (%)	Electrical efficiency (%)	Uncertainty (% , $k=2$ )	Index
100	19.4	0.16	
50	20.0	0.17	<b>1.04</b>
80	19.8	0.20	<b>1.03</b>
100	19.1	0.18	

**Test Methodology.** Systematic testing was performed to determine the parameters that affect the electrical and/or thermal performance of the fuel cell system. The influence of the following parameters was evaluated based on steady-state testing:

- Electrical power output (expressed as the fraction of the maximum output, i.e., load fraction)
- Ambient temperature
- Ambient relative humidity
- Temperature of fluid entering the fuel cell system for thermal load extraction
- Flow rate of fluid entering the fuel cell system for thermal load extraction

All steady-state testing was performed according to ASME PTC 50 [8] for fuel cell power systems, which describes the best practices for recording the efficiency of a fuel cell system.

Testing the fuel cell system proved difficult due to the larger than anticipated day-to-day performance degradation. A “bracketing” test sequence was thus employed to avoid confusing the impact of the parametric studies versus the time-dependent degradation. For steady-state testing, one test bracket was set up for each parameter. For instance, to determine the change in performance as a function of the ambient temperature, the fuel cell system performance was first measured at an ambient temperature of 35°C. Holding all other parameters constant, the ambient temperature was then changed to 5°C and the fuel cell’s steady-state performance was measured again. Finally, the ambient temperature was returned to 35°C for the last steady-state measurement. The bracket was not considered valid unless the performance measurements for the first and last tests were within the bounds of their respective uncertainties. For each valid bracket, a relative performance index was calculated that shows how the electrical or thermal performance changed. In tables that include the relative performance index, **bolded** entries indicate a statistically significant change in efficiency

$$\text{Index} = \frac{(\eta_2)}{\frac{(\eta_1 + \eta_3)}{2}} \quad (7)$$

## Test Results

Extensive testing of the fuel cell system showed that while the thermal efficiency responded to ambient temperature electrical load fraction, fluid inlet temperature, and fluid flow rate, the electrical efficiency was affected by only the electrical load fraction (i.e., the electrical power output) and the operating hours of the system.

**Electrical Load Fraction.** The electrical performance of the fuel cell system was measured at three power output levels (2.5, 4.0, and 5.0 kW) in both the grid-interconnected and grid-independent modes of operation. A four-test bracket was set up for both modes of operation, and the results are shown in Tables 3 and 4.

The relative indices for the 50% and 80% load fractions were both calculated with respect to the average of the two bracketing

**Table 4 Grid-independent electrical efficiency four-test bracket**

Load fraction (%)	Electrical efficiency (%)	Uncertainty (% , $k=2$ )	Index
100	18.7	0.17	
50	18.8	0.15	1.01
80	19.5	0.15	<b>1.04</b>
100	18.7	0.14	

100% load fraction tests. A value of 1.04, for example, demonstrates that the electrical efficiency is 4% greater than the 100% load fraction efficiency.

In the grid-interconnected mode of operation, which is the predominant mode, the electrical performance at both 50% and 80% load fractions were found to be statistically different than at the 100% load fraction (Table 3). However, there was no statistically significant difference between the 50% and 80% load fractions.

The electrical efficiency at each load fraction in the grid-independent mode of operation (Table 4) was less than the grid-interconnected mode. Additionally, in the grid-independent mode there was no significant difference between the 50% and 100% load fraction tests, but the 80% load fraction was still found to perform better than the 100% load fraction. The difference in performance between the two modes of operation at the same load fraction cannot be readily explained, but it was found to be repeatable.

**Steady-State Thermal Load.** An extensive test plan was derived to determine the effects of the thermal load upon the electrical and thermal efficiency of the fuel cell system. Three-test brackets were used. For a given bracket, either the fluid flow rate or fluid inlet temperature was varied between two levels. These brackets were assembled into sets of ten tests that incorporated each possible parameter change. The set of ten tests was performed at two different electrical load fractions and four ambient temperature/relative humidity combinations for a total of 80 tests. The resulting electrical and thermal efficiencies are shown in Table 5, respectively.

The first three columns in Table 5 indicate the bracket ID and fluid flow rate/temperature combination of the fluid used to extract the thermal load from the fuel cell. The tests were performed chronologically from top to bottom. The remaining columns are organized first by ambient temperature, then by relative humidity, and finally by electrical load fraction LF. In both tables, the efficiency and relative performance index are reported for each case. The shaded tests comprise the second test in a three-test bracket, and the surrounding unshaded tests are the first or third tests for the respective bracket. The third tests in brackets I and III are shared with the first tests of brackets II and IV, respectively. Because of the high variability in the unit’s performance, only tests within a three-test bracket can be compared, and these comparisons are expressed as relative performance indices in Table 5.

The relative performance indices are reported for the electrical and thermal efficiency of each of the valid brackets, which are brackets in which the efficiency at the first and third test differs by less than the combined measurement uncertainty for both the electrical and thermal efficiency. For example, at an ambient temperature of 35°C, a relative humidity of 75%, and an electrical load fraction of 100%, the electrical efficiencies of the first and third tests in bracket II differ by more than 2%, which is greater than the sum of the uncertainties for the electrical efficiency (Table 2). This three-test bracket is ruled invalid. Bolded indices in Table 5 indicate parameter changes that resulted in statistically significant changes in performance. An index close to unity for either the electrical or thermal efficiency indicates that the parameter change did not affect the performance.

According to the relative index for electrical efficiency in Table

**Table 5 Electrical efficiency and relative performance index for each steady-state thermal load bracket**

Bracket ID	Fluid Flow Rate (L/min)	Fluid Inlet Temp (°C)	Ambient Temperature = 35 °C								Ambient Temperature = 11.5 °C							
			Relative Humidity = 40 %				Relative Humidity = 75 %				Relative Humidity = 55 %				Relative Humidity = 25 %			
			LF = 100 %		LF = 50 %		LF = 100 %		LF = 50 %		LF = 100 %		LF = 50 %		LF = 100 %		LF = 50 %	
			$\eta_e$	Index	$\eta_e$	Index	$\eta_e$	Index	$\eta_e$	Index	$\eta_e$	Index	$\eta_e$	Index	$\eta_e$	Index	$\eta_e$	Index
I	35	55	18.0		20.1		16.8		20.2		18.6		19.5		18.5		19.5	
	5	55	18.1	1.00	20.2	1.00	16.4	0.99	20.1	0.99	18.4	0.99	b		19.0	1.03	b	
II	35	55	18.3		20.2		16.4		20.4		18.4		19.4		18.4		18.3	
	35	18	18.4	0.99	20.3	1.00	19.2	a	20.4	1.00	18.1	0.99	19.2	0.99	18.7	1.01	18.3	1.01
III	5	18	18.7		20.2		18.5		20.7		17.5		19.4		18.4		19.5	
	35	18	18.9	1.00	20.1	1.00	18.6	1.00	20.6	1.00	17.2	0.99	19.6	1.01	18.7	1.01	19.7	a
IV	5	18	19.1		20.1		18.8		20.7		17.4		19.5		18.5		19.9	
	5	55	19.0	1.00	19.9	0.99	17.8	a	20.2	a	17.5	1.02	b		18.3	0.99	b	
	5	18	18.8		20.2		17.0		20.1		17.2		19.8		18.5		19.6	

LF Electrical load fraction  
 a Invalid bracket  
 b System would not output steady current due to internal control issues. Data not valid

Bracket ID	Fluid Flow Rate (L/min)	Fluid Inlet Temp (°C)	Ambient Temperature = 35 °C								Ambient Temperature = 11.5 °C							
			Relative Humidity = 40 %				Relative Humidity = 75 %				Relative Humidity = 55 %				Relative Humidity = 25 %			
			LF = 100 %		LF = 50 %		LF = 100 %		LF = 50 %		LF = 100 %		LF = 50 %		LF = 100 %		LF = 50 %	
			$\eta_{th}$	Index	$\eta_{th}$	Index	$\eta_{th}$	Index	$\eta_{th}$	Index	$\eta_{th}$	Index	$\eta_{th}$	Index	$\eta_{th}$	Index	$\eta_{th}$	Index
I	35	55	39.2		37.2		36.8		35.9		36.6		28.9		36.8		29.6	
	5	55	10.9	0.28	21.5	0.58	10.0	0.28	21.2	0.59	11.5	0.31	b		11.6	0.31	b	
II	35	55	39.6		37.3		39.9		36.4		36.4		28.8		37.1		23.5	
	35	18	42.9	1.08	42.6	1.15	45.9	a	43.7	1.21	42.3	1.16	34.5	1.22	41.2	1.11	34.6	1.48
III	5	18	44.5		44.0		45.9		46.1		43.7		35.5		41.4		36.8	
	35	18	43.6	0.98	42.5	0.96	47.9	1.04	44.3	0.97	44.2	1.03	34.0	0.95	40.6	0.98	35.7	a
IV	5	18	44.8		44.5		46.5		45.6		42.4		35.7		41.6		37.6	
	5	55	11.5	0.26	21.4	0.48	10.8	a	22.1	a	10.9	0.25	b		11.2	0.27	b	
	5	18	44.8		45.3		45.6		45.5		44.2		37.3		41.8		38.0	

LF Electrical load fraction  
 a Invalid bracket  
 b System would not output steady current due to internal control issues. Data not valid

5, changing the thermal load does not affect the electrical performance of the fuel cell system. The thermal efficiency was, understandably, affected by changes in the thermal load, as shown in Table 5. Bracket III, which increased the flow rate at a fluid temperature of 18 °C, did not result in a statistically significant performance change. Brackets I, II, and IV did affect the thermal efficiency of the system. Large differences in thermal efficiency were observed in each of the brackets that included the 55 °C, 5 l/min test (brackets I and IV). This combination of a low flow rate and an inlet temperature near the maximum outlet temperature of the fuel cell system ( $\approx 63^\circ\text{C}$ ) prevented the full amount of thermal energy available from the fuel cell system being transferred to the fluid stream. In this case, an integral radiator on the fuel cell system dissipated the remaining thermal energy to the environment. Smaller differences are seen in bracket II, which changed the inlet temperature at the 35 l/min flow rate. These results are consistent over the eight sets of ambient conditions and electrical load fractions.

**Ambient Condition Investigation.** Test brackets were set up to determine the effect of ambient temperature and relative humidity on the electrical and thermal efficiency of the fuel cell system.

The ambient temperature and relative humidity were varied separately, and each parameter was varied at the 50% and 100% electrical load fraction. All tests were performed while extracting thermal energy from the system with the fluid flow rate and inlet temperature constant at 35 l/min and 55 °C, respectively. The test sequence and results are shown in Table 6.

Neither the ambient temperature nor the relative humidity affected the electrical efficiency, but a drop in the ambient temperature from 35 °C to 5 °C did significantly reduce the thermal efficiency. Presumably, this loss in thermal output resulted from the system redirecting thermal energy internally to maintain the proper system temperature. While no change in performance was observed at various relative humidity levels, 75% is the highest relative humidity attainable in the environmental chamber. Humidity levels closer to saturation may have affected the systems performance.

**Thermal Load Extraction Investigation.** Test brackets were devised to explicitly determine if the electrical efficiency depended upon whether or not thermal energy was extracted from the system. Brackets for 50%, 80%, and 100% load fractions were performed at ambient conditions of 11.5 °C and 55% RH. During

**Table 6 Electrical and thermal performance varying ambient environmental conditions**

Load Fraction (%)	Ambient Temperature (°C)	Ambient RH (%)	Electrical Performance		Thermal Performance	
			Efficiency (%)	Relative Index	Efficiency (%)	Relative Index
50	35	40	18.1	1.01	37.0	1.02
50	35	75	18.3		37.4	
50	35	40	18.0		36.5	
50	35	40	17.8	1.01	37.1	0.70
50	5	40	18.2		26.0	
50	35	40	18.2		37.0	
100	35	40	18.3	1.01	36.6	0.99
100	35	75	18.8		36.6	
100	35	40	18.9		37.0	
100	35	40	18.6	1.02	36.7	0.82
100	5	40	18.8		29.9	
100	35	40	18.4		36.2	

tests with thermal extraction, the fluid flow rate and inlet temperature were held constant at 35 l/min and 55°C, respectively. Table 7 shows that the electrical performance proved not to be influenced by the presence of a thermal load on the system.

**Transient Electrical Load.** The transient electrical performance of the fuel cell system was measured in the grid-interconnected and grid-independent mode. No thermal energy was extracted from the system during these tests. The electrical performance was monitored every 5 s, as opposed to a 30 s interval for steady-state tests. In the grid-interconnected mode, the fuel cell system was shifted between power levels in the 6 possible permutations:

- 50% to 80%
- 50% to 100%
- 80% to 100%

- 80% to 50%
- 100% to 80%
- 100% to 50%

In the grid-interconnected mode, the fuel cell system slowly ramps up the power output, as well as the fuel consumption, until the power reaches the setpoint. The system took between 7 min and 18 min to reach steady state after a shift. Comparing the respective entries from the third and fourth columns of Table 8, a trend emerges where transitioning to a higher load fraction results in a small dip in electrical efficiency during the transient period, whereas the opposite occurs when transitioning to a lower load fraction.

The same shifts in power were performed in the grid-independent mode. In this mode, the system uses its batteries to immediately meet the power demand and slowly ramps the fuel consumption to meet the need. The time interval required for the fuel consumption to reach steady-state conditions after the electrical load shift (Table 8) was approximately the same for both the grid-interconnected and grid-independent modes, except for the comparatively faster response time when transitioning from 100% to 50% load fractions. Finally, the trend as to the electrical efficiency during the steady-state periods versus the transitioning period, Table 8 (sixth and seventh columns) was opposite to the trend observed for the grid-interconnected mode. The change in stored energy within the batteries is not taken into account in these calculations. Figures 2 and 3 show typical traces for the electrical power output, fuel energy consumption, and electrical efficiency during a shift in load fraction.

**Table 7 Electrical performance with and without a thermal load**

Load fraction	Thermal load?	Efficiency		Overall (%)
		Electrical (%)	Thermal (%)	
50	Yes	19.8	19.4	39.2
	No	19.7	0.0	19.7
	Yes	19.8	19.3	39.2
80	Yes	20.0	28.1	48.1
	No	20.0	0.0	20.0
	Yes	20.0	28.2	48.2
100	Yes	18.9	32.1	51.0
	No	19.0	0.0	19.0
	Yes	19.0	32.1	51.0

**Quasi-Steady Fluid Inlet Temperature.** The thermal performance of the fuel cell system was monitored while the thermal fluid inlet temperature was slowly increased; i.e., “quasi-steady.” The fluid temperature increased slowly enough to assume a rela-

**Table 8 Electrical performance during shifts in electrical load fraction**

Steady Electrical Load Fraction	Transition	Grid-Interconnected		Grid-Independent	
		Electrical Efficiency (%)	Duration (min)	Electrical Efficiency (%)	Duration (min)
50	50 to 100	19.4	18	19.2	18
100		18.4		20.1	
100	100 to 80	18.7	9	18.9	6
80		19.5		18.8	
80	80 to 50	19.6	8	19.8	6
50		19.8		17.9	
50	50 to 80	19.8	7	19.3	9
80		19.2		20.7	
80	80 to 100	19.8	9	19.7	10
100		18.7		18.9	
100	100 to 50	19.2	18	18.8	7
50		20.1		16.2	
50		20.2		19.2	

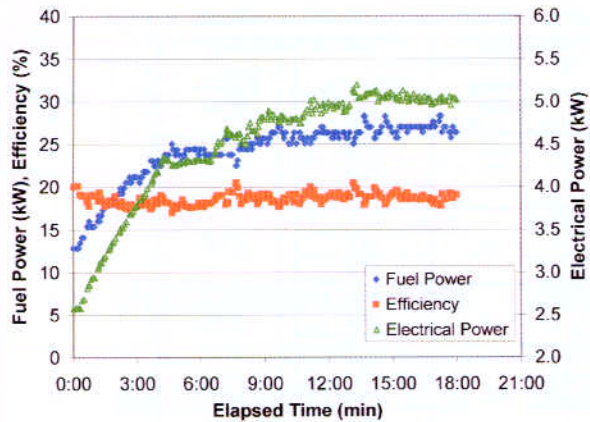


Fig. 2 Performance during a 50% to 100% shift in grid-interconnected mode

tively steady temperature, but the rise in fluid temperature provided a detailed picture of the system's performance as a function of temperature. The fuel cell system was used to heat approximately 1000 l of fluid until the fluid temperature no longer increased. This test was performed at the 50%, 80%, and 100% load fractions at three different fluid flow rates (5, 20, and 35 l/min). Figure 4 shows the results of all these tests. All of the 80% and 100% load fraction tests show a dramatic knee in the curve, which results when the fluid outlet temperature reaches its maximum value (~63°C). At each load fraction, the respective curves for the 20 and 35 l/min tests are nearly identical, and the curves at the 5 l/min tests bend downward earlier than the other tests at the same load fraction.

#### Residential Space and Domestic Hot Water Heating Loads.

The fuel cell system was used to heat a thermal storage tank through an internal heat exchanger, as discussed above. The thermal storage tank was used to supply hot water for a domestic water heater and, separately, thermal energy for space heating loads. The tests simulating domestic hot water usage were performed according to the DOE test procedure for water heaters [10]. The space heating loads are representative of the maximum heating day from a typical single-family home in Atlanta, GA, which was modeled using the building energy simulation program DOE2 [11].

The test simulating the domestic hot water load showed that this particular fuel cell system's ability to supply thermal energy far exceeds the thermal energy requirements for a typical residen-

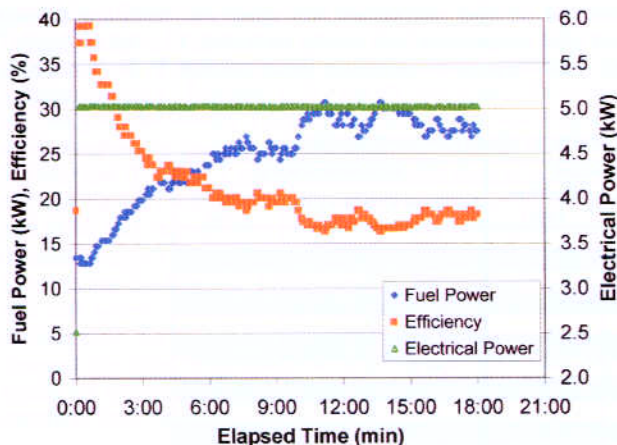


Fig. 3 Performance during a 50% to 100% shift in grid-independent mode

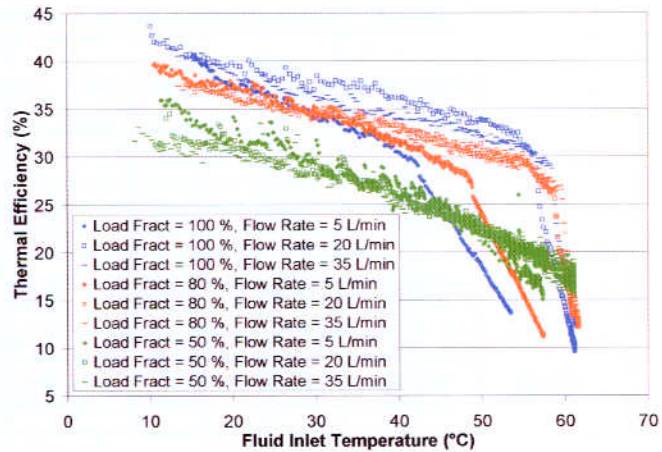


Fig. 4 Quasi-steady fluid inlet temperature test

tial hot water load. The overall efficiencies were approximately 32% for the 50% electrical load fraction and only 24% for the 100% load fraction (Table 9). In a field test of a residential fuel cell providing electricity and domestic hot water, Boettner [6] measured an overall efficiency of 29.7% (LHV).

At an overall efficiency of 43%, the fuel cell was much more efficient supplying the space heating loads. The heat exchanger in the thermal storage tank did limit the fuel cell system from meeting larger space heating loads. Figure 5 shows the space heating loads used and the temperature entering and leaving the storage tank on an hourly basis. The results from the space heating load test will be used to evaluate the model developed as part of the rating methodology.

**Performance Degradation.** The electrical and thermal efficiency of the unit changed with cumulative hours of operation.

Table 9 Real-world thermal load test efficiencies (average of three 24 h tests)

Efficiency	Load Fraction		
	Domestic hot water load		Space heating load
	50%	100%	100%
Electrical	18.1	17.2	19.5
Thermal	13.7	6.6	23.6
Overall	31.8	23.8	43.2

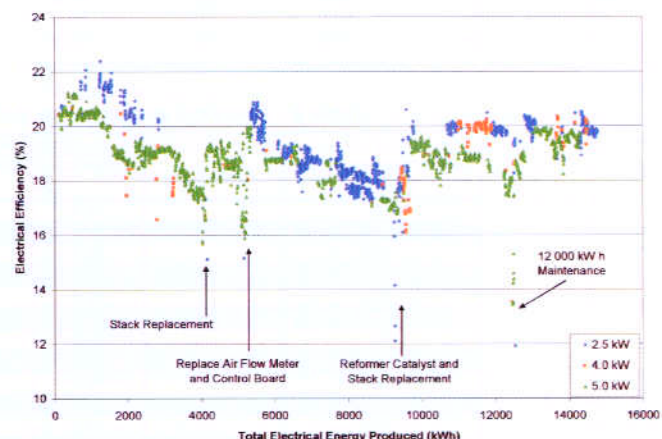


Fig. 5 Electrical performance degradation

The degradation was significant enough to warrant two stack changes, which were diagnosed by the manufacturer, over the warranty period of the unit. Upon installing the third stack, the manufacturer replaced a reformer catalyst, and the degradation rate was significantly reduced. Figure 5 shows the electrical efficiency of the unit as a function of the cumulative runtime. Incorporating the performance degradation in the rating methodology will be important until manufacturers extend the lifetime of such units.

## Conclusion

The performance of the residential-scale stationary fuel cell tested depends upon the environmental, electrical, and thermal load applied to the unit. Specifically, the electrical load fraction and cumulative runtime affected the electrical efficiency. The thermal efficiency depends upon the ambient temperature, electrical load fraction, fluid inlet temperature, and fluid flow rate. When used to supply typical thermal loads in a residential application, the thermal energy requirement of each load greatly affected the overall efficiency of the unit. For a typical residential water heating load, the fuel cell's overall efficiency was less than 32%, but for a residential space heating load, the overall efficiency was 43%. However, the overall efficiency could be as high as 68% if all of the thermal energy produced by the system could be utilized.

The application of the fuel cell unit will greatly affect its operating efficiency. Therefore, consumers considering the economic benefits of such a unit will need a rating methodology that accurately captures the full range of performance for these systems. The data collected by NIST will provide a basis for the formation of such a rating methodology. Additional fuel cell units are being tested, and future results will be used to expand and refine the proposed rating methodology.

## Acknowledgment

The authors are grateful to Gerald Caesar of the Advanced Technology Program for funding this work. We would like to thank Luis Luyo and Rusty Hettenhouser whose hard work and skill were essential in the construction and maintenance of the fuel cell test facility.

## Nomenclature

### Uppercase

- $E$  = energy flow to/from fuel cell unit (kJ)  
 Index = relative performance metric: results of the middle test versus the two bracketing tests  
 $P$  = pressure of natural gas at the gas meter (Pa)

$T$  = temperature of the heat transfer fluid or natural gas (K)

$V$  = volume of fluid into/out of the fuel cell unit ( $m^3$ )

### Lowercase

- $c_p$  = specific heat of heat transfer fluid (kJ/kg K)  
 $e$  = higher heating value of natural gas (kJ/ $m^3$ )

### Greek

- $\eta$  = efficiency of the fuel cell unit (%)  
 $\rho$  = density of heat transfer fluid (kg/ $m^3$ )

### Subscripts

- 1,2,3 = first, second, or third test in a three-test bracket  
 avg = average of inlet and outlet heat transfer fluid streams  
 fuel = indicates a property of the natural gas stream  
 HTF = indicates a property of the heat transfer fluid  
 $i$  = index of measurement scans  
 inlet = HTF property at the inlet to fuel cell unit  
 outlet = HTF property at the outlet from fuel cell unit

## References

- [1] Bullock, D., Atul, K., and Rabago, K., 2005, "Are Stationary Fuel Cells Ready for Market?," *Fuel Cell Magazine*, **4**(6), pp. 16–18.
- [2] Williams, M., Utz, B., and Moore, K., 2004, "DOE FE Distributed Generation Program," *J. Fuel Cell Sci. Technol.*, **1**, pp. 18–20.
- [3] Ellis, M. W., and Gunes, M. B., 2002, "Status of Fuel Cell Systems for Combined Heat and Power Applications in Buildings," *ASHRAE Trans.*, **108**(1), pp. 1032–1044.
- [4] U. S. Department of Defense, 2005, U. S. DOD fuel cell demonstration program home page, cited Feb 18, 2005, available at [http://www.dodfuelcell.com/res/site\\_performance.php4](http://www.dodfuelcell.com/res/site_performance.php4)
- [5] Gigliucci, G. et al., 2004, "Demonstration of a Residential CHP System Based on PEM Fuel Cells," *J. Power Sources*, **131**, pp. 62–68.
- [6] Boettner, D., Massie, C., and Massie, D., 2004, "Lessons Learned from Residential Experience with Proton Exchange Membrane Fuel Cell Systems for Combined Heat and Power," *Proceedings of the ASME Fuel Cell Science, Engineering, and Technology Conference*, pp. 267–272.
- [7] Holcomb, F., Davenport, B., Joselick, N., and Binder, M., 2004, "Results of a Residential Proton Exchange Membrane (PEM) Fuel Cell Demonstration at a Military Facility in New York," *ASHRAE Trans.*, **110**(1), pp. 25–32.
- [8] ASME PTC 50-2002, "Fuel Cell Power Systems Performance," 2002, American Society of Mechanical Engineers, New York.
- [9] Davis, M., and Fanney, A., 2003, "Test Facility for Determining the Seasonal Performance of Residential Fuel Cell Systems," *Proceedings of the Hydrogen and Fuel Cells 2003 Conference and Trade Show*, Vancouver, BC, June 8–11.
- [10] U. S. Department of Energy-Office of Energy Efficiency and Renewable Energy, 1998, "Energy Conservation Program for Consumer Products: Uniform Test Method for Measuring the Energy Consumption of Water Heaters," 10 CFR Part 430, Appendix E to Subpart B of Part 430.
- [11] Gunes, B., and Ellis, M., 2003, "Evaluation of Energy, Environmental, and Economic Characteristics of Fuel Cell Combined Heat and Power Systems for Residential Applications," *ASME J. Energy Resour. Technol.*, **125**, pp. 208–220.